

Article

Synthesis and Biological Evaluation of Benzo [4,5]- and Naphtho[2',1':4,5]imidazo[1,2-c]pyrimidinone Derivatives

Polina Kamzeeva ^{1,†}, Nikolai Dagaev ^{2,†}, Sofia Lizunova ³, Yuri Khodarovich ^{1,4} , Anna Sogomonyan ¹ , Anastasia Kolchanova ², Vadim Pokrovsky ^{5,6} , Vera Alferova ¹ , Alexey Chistov ¹, Artur Eshtukov-Shcheglov ¹, Elizaveta Eshtukova-Shcheglova ⁷ , Evgeny Belyaev ⁸, Dmitry Skvortsov ^{2,*}, Anna Varizhuk ^{3,9,10} and Andrey Aralov ^{1,3,10,*} 

- ¹ Shemyakin-Ovchinnikov Institute of Bioorganic Chemistry, Russian Academy of Sciences, 117997 Moscow, Russia; polinabast@yandex.ru (P.K.)
 - ² Department of Chemistry and Faculty of Bioengineering and Bioinformatics, Lomonosov Moscow State University, 119991 Moscow, Russia; nikolas.dagaev@yandex.ru (N.D.)
 - ³ Lopukhin Federal Research and Clinical Center of Physical-Chemical Medicine of Federal Medical Biological Agency, 119435 Moscow, Russia
 - ⁴ Research and Educational Resource Center for Cellular Technologies, The Peoples' Friendship University of Russia, 117198 Moscow, Russia
 - ⁵ N.N. Blokhin Cancer Research Center, 115478 Moscow, Russia
 - ⁶ Research Institute of Molecular and Cellular Medicine, RUDN University, 117198 Moscow, Russia
 - ⁷ Lomonosov Institute of Fine Chemical Technology, MIREA-Russian Technological University, 119571 Moscow, Russia
 - ⁸ Frumkin Institute of Physical Chemistry and Electrochemistry, Russian Academy of Sciences, 119071 Moscow, Russia
 - ⁹ Moscow Institute of Physics and Technology, 141701 Dolgoprudny, Russia
 - ¹⁰ G4_Interact, USERN, University of Pavia, 27100 Pavia, Italy
- * Correspondence: skvorratd@mail.ru (D.S.); baruh238@mail.ru (A.A.)
† These authors contributed equally to this work.



Citation: Kamzeeva, P.; Dagaev, N.; Lizunova, S.; Khodarovich, Y.; Sogomonyan, A.; Kolchanova, A.; Pokrovsky, V.; Alferova, V.; Chistov, A.; Eshtukov-Shcheglov, A.; et al. Synthesis and Biological Evaluation of Benzo [4,5]- and Naphtho[2',1':4,5]imidazo[1,2-c]pyrimidinone Derivatives. *Biomolecules* **2023**, *13*, 1669. <https://doi.org/10.3390/biom13111669>

Academic Editors: Chandra Mishra and Mohd Abdullah

Received: 16 October 2023

Revised: 13 November 2023

Accepted: 15 November 2023

Published: 20 November 2023



Copyright: © 2023 by the authors. Licensee MDPI, Basel, Switzerland. This article is an open access article distributed under the terms and conditions of the Creative Commons Attribution (CC BY) license (<https://creativecommons.org/licenses/by/4.0/>).

Abstract: Azacarbazoles have attracted significant interest due to their valuable properties, such as anti-pathogenic and antitumor activity. In this study, a series of structurally related tricyclic benzo[4,5]- and tertacyclic naphtho[2',1':4,5]imidazo[1,2-c]pyrimidinone derivatives with one or two positively charged tethers were synthesized and evaluated for anti-proliferative activity. Lead tetracyclic derivative **5b** with two amino-bearing arms inhibited the metabolic activity of A549 lung adenocarcinoma cells with a CC₅₀ value of 3.6 μM, with remarkable selectivity (SI = 17.3) over VA13 immortalized fibroblasts. Cell-cycle assays revealed that **5b** triggers G2/M arrest without signs of apoptosis. A study of its interaction with various DNA G4s and duplexes followed by dual luciferase and intercalator displacement assays suggests that intercalation, rather than the modulation of G4-regulated oncogene expression, might contribute to the observed activity. Finally, a water-soluble salt of **5b** was shown to cause no acute toxic effects, changes in mice behavior, or any decrease in body weight after a 72 h treatment at concentrations up to 20 mg/kg. Thus, **5b** is a promising candidate for studies in vivo; however, further investigations are needed to elucidate its molecular target(s).

Keywords: imidazopyrimidinone; anti-proliferative activity; azacarbazoles; cytostatic agent

1. Introduction

Cancer is a life-threatening disease that causes millions of deaths worldwide annually [1]. Chemotherapy represents a significant treatment option for cancer, and it stimulates the ongoing search for new therapeutic agents [2]. Carbazole and its benzo- and aza-derivatives exhibit notable antitumor activity [3–8]. They demonstrate a variety of mechanisms of action, including the inhibition of tubulin polymerization [9,10] and DNA-binding enzymes [11–13] (Figure 1A–C). A carbazole derivative, BMVC, possesses

an ability to stabilize telomeric G-quadruplex (G4) structures and thus inhibits telomerase activity, which is responsible for cell immortalization [11,14] (Figure 1D). Carbazole-based derivatives are also able to stabilize G4s in the cMyc promoter, resulting in the inhibition of oncogene transcription [15]. Compounds with the γ -carboline scaffold intercalate into duplex DNA and regulate the activity of topoisomerase II [12,13,16,17] (Figure 1E). The cellular targets of other antitumor carbazole-based derivatives remain unknown and are still to be investigated [18].

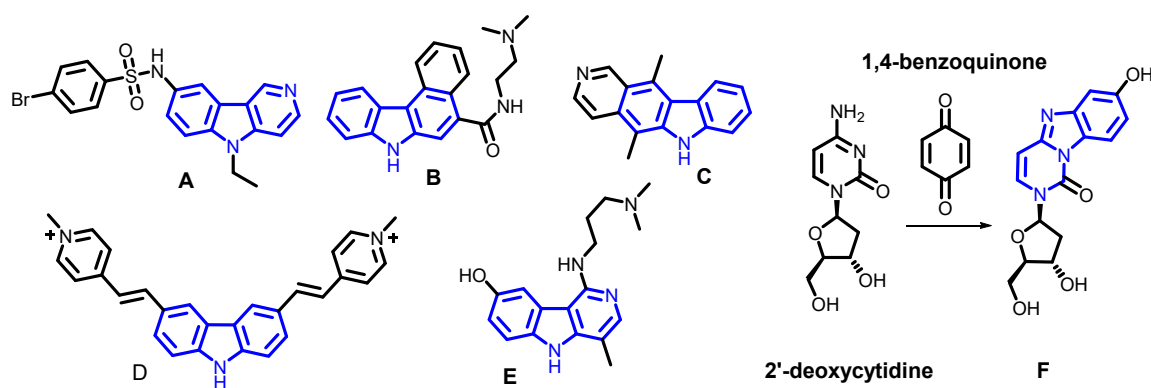


Figure 1. Examples of derivatives of γ -carboline (A,E) and carbazole (B–D). An example of synthesis of the adduct of 2'-deoxycytidine with 1,4-benzoquinone (F). Blue scaffolds are γ -carboline and carbazole.

More than 30 years ago, an adduct of 2'-deoxycytidine with 1,4-benzoquinone was synthesized during the investigation of the cancerogenic properties of benzene [19] (Figure 1F). However, a biological evaluation of this heteroaromatic scaffold was not performed. Taking into account the intriguing antitumor activity of γ -carbolines, we decided to evaluate this property for a set of compounds with a benzo[4,5]imidazo[1,2-c]pyrimidinone scaffold. Since DNA fragments are considered the main target of most γ -carbolines, we designed compounds in a way that allows them to effectively interact with DNA structures. In particular, the chosen planar aromatic system, supposed to stabilize duplex and G4 DNA structures via stacking interactions, was expanded to naphtho[2',1':4,5]imidazo[1,2-c]pyrimidinone in order to enhance stabilization efficiency [20,21]. Moreover, basic side chains were introduced into the compounds to provide electrostatic interaction with the negatively charged DNA sugar-phosphate backbone [20,21]. In addition to the unmodified amino group, guanidino- and dimethylamino-containing substituents were proposed due to their higher basicity. The choice of the aforementioned modifications is supported by their successful application in the design of carbazole- and γ -carboline-based derivatives with antitumor activity [5,12,16]. Thus, we synthesized a series of benzo[4,5]- and naphtho[2',1':4,5]imidazo[1,2-c]pyrimidinones with one or two positively charged tethers. Their cytotoxicity and selectivity of action was evaluated on cell lines of cancerous and non-cancerous etiology, and possible DNA-related mechanisms of action were investigated.

2. Materials and Methods

1,8-Diazabicyclo[5.4.0]undec-7-ene (DBU) and 37% aqueous CH_2O were purchased from Thermo Fisher Scientific (Madison, WI, USA). 1,4-Benzoquinone, 1,4-naphthoquinone, methyl 2-bromoacetate, ethane-1,2-diamine, 1H-pyrazole-1-carboxamide hydrochloride, and sodium cyanoborohydride were obtained from Sigma-Aldrich (St. Louis, MO, USA). Solvents were purchased from commercial sources and used without further purification, except for CH_2Cl_2 , which was distilled over calcium hydride. Thin layer chromatography (TLC) was performed on plates (Merck, Darmstadt, Germany) pre-coated with silica gel (60 mm, F₂₅₄) and visualized using UV light (254 and 365 nm). Column chromatography (CC) was performed on silica gel (0.040–0.063 mm, Merck, Germany). Volatiles were evaporated on a Heidolph Hei-VAP Precision ML/G3B rotary evaporator (Schwabach,

Germany). ^1H and ^{13}C spectra were recorded on a Bruker Avance III 600 spectrometer (Bruker, Rheinstetten, Germany) at 600 and 150 MHz, respectively, or on a Bruker Fourier 300 (Bruker, Rheinstetten, Germany) at 300 and 75 MHz, respectively, at 303 K. Chemical shifts are reported in δ (ppm) units using residual ^1H signals from deuterated solvents as references. Multiplicity is reported using the following abbreviations: s (singlet), d (doublet), t (triplet), m (multiplet), and br (broad). Coupling constants (J) are given in Hz. HRMS analysis was performed using a Thermo LTQ Orbitrap XL ion trap instrument in positive ion mode (ESI+, 150–2000 au). The preparative HPLC purification of compounds **6a,b** and **7a,b** was performed on an Interchim Puriflash 4250 preparative chromatograph using a VDSphere 100 C18-E 250 \times 20 mm, 5 μm column. CH_3CN (with 0.1% TFA) and aq. TFA (0.1%) were used as eluents. UV-vis detection was performed at 210 nm, 254 nm, 350 nm, and 400 nm. A linear gradient from 5 to 95% of CH_3CN in 10 min, followed by 4 min of 95% CH_3CN at 20 mL/min flow rate, was used. Fractions containing the target compound were collected, organic solvent was removed in vacuo, and water was lyophilized. The HPLC purity analysis was performed using an Agilent 1260 Infinity II instrument. LC parameters: flow 1 mL/min on a Macherey Nagel Nucleodur Gravity column C18 EC (4.6 \times 250 mm, 5 μm) and gradient elution method. Mobile phases: A—aq. TFA (0.1%), B— CH_3CN (with 0.1% TFA). Gradient program: 0–10 min from 5 to 95% B, 10–14 min 95% B. UV detection wavelengths: 225, 254, 350, and 400 nm. Methyl 4-amino-2-oxo-1(2H)-pyrimidine acetate **1** was prepared according to the reported procedure [22].

2.1. Chemical Synthesis

2.1.1. Methyl 2-(7-Hydroxy-1-oxobenzo[4,5]imidazo[1,2-c]pyrimidin-2(1H)-yl)acetate **2a**

To a suspension of methyl 4-amino-2-oxo-1(2H)-pyrimidine, acetate **1** (390 mg, 2.12 mmol) in 0.1 M sodium acetate buffer (50 mL, pH 4.5), 1,4-benzoquinone (960 mg, 8.90 mmol, 4.2 eq.) was added, and the resulting mixture was stirred at 37 $^\circ\text{C}$ for 24 h. The mixture was evaporated in vacuo, co-evaporated with CH_3CN (2 \times 10 mL), and subjected to column chromatography with dry loading on silica gel (0 \rightarrow 3% CH_3OH in CH_2Cl_2), yielding **2a** as a brownish amorphous solid (347 mg, 1.27 mmol, 60%).

^1H NMR (300 MHz, $\text{DMSO}-d_6$): δ 9.63 (br s, 1H), 7.72 (d, $J = 2.4$ Hz, 1H), 7.61 (d, $J = 7.8$ Hz, 1H), 7.56 (d, $J = 8.7$ Hz, 1H), 6.97 (dd, $J = 8.7$ Hz, $J = 2.4$ Hz, 1H), 6.69 (d, $J = 7.8$ Hz, 1H), 4.83 (s, 2H), 3.74 (s, 3H). ^{13}C NMR (75 MHz, $\text{DMSO}-d_6$): δ 168.4, 154.2, 147.1, 137.0, 136.2, 130.0, 118.8, 115.5, 114.9, 100.3, 97.2, 52.3, 49.2. HRMS (ESI) m/z : calcd for $\text{C}_{13}\text{H}_{12}\text{N}_3\text{O}_4^+$ $[\text{M}+\text{H}]^+$: 274.0822; found 274.0820.

2.1.2. Methyl 2-(5-Hydroxy-11-oxonaphtho[2',1':4,5]imidazo[1,2-c]pyrimidin-10(11H)-yl)acetate **2b**

To a suspension of methyl 4-amino-2-oxo-1(2H)-pyrimidine, acetate **1** (765 mg, 4.18 mmol) in a mixture of 0.1 M sodium acetate buffer (100 mL, pH 4.5) and $\text{C}_2\text{H}_5\text{OH}$ (50 mL), 1,4-naphthoquinone (2.64 g, 16.7 mmol, 4.0 eq.) was added, and the resulting mixture was stirred at 50 $^\circ\text{C}$ for 7 days. The mixture was evaporated in vacuo, co-evaporated with CH_3CN (2 \times 10 mL), and subjected to column chromatography with dry loading on silica gel (0 \rightarrow 3% CH_3OH in CH_2Cl_2), yielding **2b** as a brown amorphous solid (284 mg, 0.88 mmol, 21%).

^1H NMR (600 MHz, $\text{DMSO}-d_6$): δ 10.40 (s, 1H), 8.50 (d, $J = 8.2$ Hz, 1H), 8.29 (d, $J = 8.2$ Hz, 1H), 7.89 (s, 1H), 7.69 (ddd, $J = 1.2$ Hz, $J = 6.9$ Hz, $J = 8.2$ Hz, 1H), 7.59 (d, $J = 7.8$ Hz, 1H), 7.58 (ddd, $J = 1.2$ Hz, $J = 6.9$ Hz, $J = 8.2$ Hz, 1H), 6.84 (d, $J = 7.8$ Hz, 1H), 4.87 (s, 2H), 3.75 (s, 3H). ^{13}C NMR (150 MHz, $\text{DMSO}-d_6$): δ 168.5, 150.5, 147.4, 145.7, 135.4, 132.6, 127.0, 126.1, 125.6, 124.9, 123.6, 123.0, 121.9, 97.8, 95.9, 52.3, 49.4. HRMS (ESI) m/z : calcd for $\text{C}_{17}\text{H}_{14}\text{N}_3\text{O}_4^+$ $[\text{M}+\text{H}]^+$: 324.0979; found 324.0978.

2.1.3. General Procedure for the Preparation of Ligands **3** with One Amino-Containing Tether

To a solution of **2** (0.1 mmol) in CH₃OH (5 mL), ethane-1,2-diamine (67 µL, 1.0 mmol, 10 eq.) was added, and the reaction mixture was stirred at 50 °C for 48 h. The mixture was evaporated to dryness, triturated with CH₂Cl₂ (5 mL), and filtered, affording **3**.

N-(2-Aminoethyl)-2-(7-hydroxy-1-oxobenzo[4,5]imidazo[1,2-c]pyrimidin-2(1H)-yl)acetamide **3a**

Starting from **2a**, the title compound was obtained with a yield of 83% as a brownish amorphous solid. ¹H NMR (300 MHz, DMSO-*d*₆): δ 8.21 (t, J = 5.6 Hz, 1H), 7.72 (d, J = 2.4 Hz, 1H), 7.54 (d, J = 7.8 Hz, 1H), 7.50 (d, J = 8.7 Hz, 1H), 6.94 (dd, J = 8.7 Hz, J = 2.4 Hz, 1H), 6.60 (d, J = 7.8 Hz, 1H), 4.59 (s, 2H), 3.14 (dt, J = 6.4 Hz, J = 5.6 Hz, 2H), 2.64 (t, J = 6.4 Hz, 2H). ¹³C NMR (75 MHz, DMSO-*d*₆): δ 166.6, 153.8, 147.5, 147.4, 137.1, 137.1, 130.3, 118.9, 114.5, 100.3, 97.0, 50.3, 41.7, 40.8. HRMS (ESI) *m/z*: calcd for C₁₄H₁₆N₅O₃⁺ [M+H]⁺: 302.1248; found 302.1247.

N-(2-Aminoethyl)-2-(5-hydroxy-11-oxonaphtho[2',1':4,5]imidazo[1,2-c]pyrimidin-10(11H)-yl)acetamide **3b**

Starting from **2b**, the title compound was obtained with a yield of 80% as a brownish amorphous solid. ¹H NMR (600 MHz, DMSO-*d*₆): δ 8.49 (d, J = 8.0 Hz, 1H), 8.30–8.24 (m, 2H), 7.91 (s, 1H), 7.68 (dd, J = 8.0 Hz, J = 7.0 Hz, 1H), 7.57 (dd, J = 8.3 Hz, J = 7.0 Hz, 1H), 7.53 (d, J = 7.2 Hz, 1H), 6.78 (d, J = 7.2 Hz, 1H), 4.64 (s, 2H), 3.18–3.09 (m, 2H), 2.66–2.62 (m, 2H). ¹³C NMR (150 MHz, DMSO-*d*₆): δ 166.6, 150.1, 147.6, 146.1, 135.9, 133.0, 126.8, 126.1, 125.7, 124.6, 123.5, 123.0, 121.9, 97.5, 96.1, 50.5, 41.9, 40.9. HRMS (ESI) *m/z*: calcd for C₁₈H₁₈N₅O₃⁺ [M+H]⁺: 352.1404; found 352.1404.

2.1.4. General Procedure for the Preparation of Intermediates **4**

To a solution of **2** (0.7 mmol) in CH₂Cl₂ (20 mL), DBU (210 µL, 1.40 mmol, 2.0 eq.) was added at room temperature, followed by the addition of methyl 2-bromoacetate (100 µL, 1.05 mmol, 1.5 eq.). The reaction mixture was kept at room temperature for 1 h, and then DBU (210 µL, 1.40 mmol, 2.0 eq.) and methyl 2-bromoacetate (100 µL, 1.05 mmol, 1.5 eq.) were added sequentially. The addition was repeated once. After 1 h, the organic layer was washed with 5% aqueous citric acid solution (2 × 20 mL) and evaporated in vacuo. The residue was purified using column chromatography on silica gel (0→1% CH₃OH in CH₂Cl₂), yielding **4**.

Methyl 2-(7-(2-methoxy-2-oxoethoxy)-1-oxobenzo[4,5]imidazo[1,2-c]pyrimidin-2(1H)-yl)acetate **4a**

Starting from **2a**, the title compound was obtained with a yield of 43% as a brownish amorphous solid. ¹H NMR (300 MHz, CDCl₃): δ 7.92 (d, J = 2.5 Hz, 1H), 7.75 (d, J = 8.9 Hz, 1H), 7.22 (m, 2H), 6.77 (d, J = 7.8 Hz, 1H), 4.74 (s, 2H), 4.74 (s, 2H), 3.83 (s, 3H), 3.82 (s, 3H). ¹³C NMR (75 MHz, CDCl₃): δ 169.0, 167.6, 155.5, 147.7, 147.1, 136.6, 136.5, 130.1, 119.2, 116.5, 100.0, 98.1, 66.0, 53.0, 52.3, 49.7. HRMS (ESI) *m/z*: calcd for C₁₆H₁₆N₃O₆⁺ [M+H]⁺: 346.1034; found 346.1033.

Methyl 2-(5-(2-methoxy-2-oxoethoxy)-11-oxonaphtho[2',1':4,5]imidazo[1,2-c]pyrimidin-10(11H)-yl)acetate **4b**

Starting from **2b**, the title compound was obtained with a yield of 48% as a brownish amorphous solid. ¹H NMR (600 MHz, DMSO-*d*₆): δ 8.53 (d, J = 8.2 Hz, 1H), 8.36 (d, J = 8.2 Hz, 1H), 7.79 (s, 1H), 7.75 (t, J = 7.6 Hz, 1H), 7.66 (t, J = 7.6 Hz, 1H), 7.64 (d, 7.8 Hz, 1H), 6.88 (d, J = 7.8 Hz, 1H), 5.08 (s, 2H), 4.88 (s, 2H), 3.76 (s, 3H), 3.75 (s, 3H). ¹³C NMR (150 MHz, DMSO-*d*₆): δ 168.9, 168.5, 150.2, 147.4, 146.6, 135.8, 134.4, 127.5, 125.6, 125.5, 125.3, 123.7, 122.6, 122.0, 98.0, 94.3, 65.5, 52.4, 51.9, 49.5. HRMS (ESI) *m/z*: calcd for C₂₀H₁₈N₃O₆⁺ [M+H]⁺: 396.1190; found 396.1188.

2.1.5. General Procedure for the Preparation of Derivatives 5 with Two Amino-Containing Tethers

To a solution of **4** (0.3 mmol) in CH₃OH (20 mL), ethane-1,2-diamine (400 µL, 6.0 mmol) was added, and the reaction mixture was stirred at 50 °C for 48 h. The mixture was evaporated to dryness, triturated with CH₂Cl₂ (10 mL), and filtered, affording **5**.

N-(2-Aminoethyl)-2-(7-(2-((2-aminoethyl)amino)-2-oxoethoxy)-1-oxobenzo[4,5]imidazo[1,2-c]pyrimidin-2(1H)-yl)acetamide **5a**

Starting from **4a**, the title compound was obtained with a yield of 91% as a beige amorphous solid. HPLC rt 5.5 min. ¹H NMR (300 MHz, DMSO-*d*₆): δ 8.32 (t, J = 5.2 Hz, 1H), 8.20 (t, J = 5.6 Hz, 1H), 7.89 (d, J = 2.4 Hz, 1H), 7.67 (d, J = 8.8 Hz, 1H), 7.59 (d, J = 7.8 Hz, 1H), 7.18 (dd, J = 8.8 Hz, J = 2.4 Hz, 1H), 6.66 (d, J = 7.8 Hz, 1H), 4.63 (s, 2H), 4.55 (s, 2H), 3.27–3.14 (m, 4H), 2.73–2.64 (m, 4H). ¹³C NMR (75 MHz, DMSO-*d*₆): δ 167.7, 166.7, 154.1, 148.4, 147.3, 138.6, 137.8, 130.0, 119.0, 114.5, 99.9, 97.0, 67.7, 50.4, 48.4, 40.8, 40.7, 40.2. HRMS (ESI) *m/z*: calcd for C₁₈H₂₄N₇O₄⁺ [M+H]⁺: 402.1884; found 402.1882.

N-(2-Aminoethyl)-2-(5-(2-((2-aminoethyl)amino)-2-oxoethoxy)-11-oxonaphtho[2',1':4,5]imidazo[1,2-c]pyrimidin-10(11H)-yl)acetamide **5b**

Starting from **4b**, the title compound was obtained with a yield of 90% as a beige amorphous solid. HPLC rt 6.3 min. ¹H NMR (600 MHz, DMSO-*d*₆): δ 8.53 (d, J = 8.1 Hz, 1H), 8.48 (d, J = 8.3 Hz, 1H), 8.27 (t, J = 5.2 Hz, 1H), 8.22 (t, J = 5.4 Hz, 1H), 7.88 (s, 1H), 7.75 (dd, J = 8.1 Hz, J = 7.0 Hz, 1H), 7.65 (dd, J = 8.3 Hz, J = 7.0 Hz, 1H), 7.59 (d, J = 7.7 Hz, 1H), 6.82 (d, J = 7.7 Hz, 1H), 4.77 (s, 2H), 4.66 (s, 2H), 3.24–3.17 (m, 2H), 3.15–3.10 (m, 2H), 2.66 (t, J = 6.3 Hz, 2H), 2.62 (t, J = 5.9 Hz, 2H). ¹³C NMR (150 MHz, DMSO-*d*₆): δ 167.2, 166.5, 150.3, 147.5, 146.9, 136.5, 134.3, 127.3, 125.5, 125.5, 125.3, 123.6, 123.0, 121.9, 97.4, 94.7, 67.8, 50.6, 42.3, 41.7, 41.1, 41.0. HRMS (ESI) *m/z*: calcd for C₂₂H₂₆N₇O₄⁺ [M+H]⁺: 452.2041; found 452.2040.

2.1.6. General Procedure for the Preparation of Di-Trifluoroacetate Salt of Derivatives 6 Bearing Two Dimethylamino-Containing Tethers

To a solution of **5** (0.05 mmol), HOAc (60 µL) and 37% aqueous CH₂O (20 µL, 0.25 mmol) in MeOH (5 mL), NaCNBH₃ (19.0 mg, 0.3 mmol) was added in small portions with vigorous stirring at 0 °C. After stirring for 2 h at room temperature, MeOH was evaporated. The residue was diluted with water (4 mL) and purified using preparative HPLC, yielding **6**.

Ditrifluoroacetate salt of N-(2-(dimethylamino)ethyl)-2-(7-(2-((2-(dimethylamino)ethyl)amino)-2-oxoethoxy)-1-oxobenzo[4,5]imidazo[1,2-c]pyrimidin-2(1H)-yl)acetamide **6a**

Starting from **5a**, the title compound was obtained with a yield of 38% as a pale yellow amorphous solid. HPLC rt 5.7 min. ¹H NMR (600 MHz, DMSO-*d*₆): δ 8.59 (t, J = 5.8 Hz, 1H), 8.48 (t, J = 5.8 Hz, 1H), 7.87 (d, J = 2.5 Hz, 1H), 7.69 (d, J = 8.8 Hz, 1H), 7.66 (d, J = 7.8 Hz, 1H), 7.21 (dd, J = 8.8 Hz, J = 2.5 Hz, 1H), 6.69 (d, J = 7.8 Hz, 1H), 4.70 (s, 2H), 4.60 (s, 2H), 3.51 (dt, J = 5.8 Hz, J = 6.0 Hz, 1H), 3.47 (dt, J = 5.8 Hz, J = 6.0 Hz, 1H), 3.14 (t, J = 6.0 Hz, 1H), 3.10 (t, J = 6.0 Hz, 1H), 2.75 (s, 6H), 2.74 (s, 6H). ¹³C NMR (150 MHz, DMSO-*d*₆): δ 168.3, 167.3, 154.1, 148.4, 147.4, 138.7, 137.8, 130.0, 119.2, 114.6, 99.8, 97.2, 67.6, 55.8, 55.5, 42.4, 42.4, 34.2, 33.8. HRMS (ESI) *m/z*: calcd for C₂₂H₃₂N₇O₄⁺ [M+2H]²⁺: 229.6292; found 229.6291.

Ditrifluoroacetate salt of N-(2-(dimethylamino)ethyl)-2-(5-(2-((2-(dimethylamino)ethyl)amino)-2-oxoethoxy)-11-oxonaphtho[2',1':4,5]imidazo[1,2-c]pyrimidin-10(11H)-yl)acetamide **6b**

Starting from **5b**, the title compound was obtained with a yield of 33% as a pale yellow amorphous solid. HPLC rt 6.5 min. ¹H NMR (600 MHz, DMSO-*d*₆): δ 8.54 (d, J = 8.0 Hz, 1H), 8.47 (d, J = 8.4 Hz, 1H), 8.25 (t, J = 5.2 Hz, 1H), 8.15 (t, J = 5.4 Hz, 1H), 7.89 (s, 1H), 7.76 (dd, J = 8.0 Hz, J = 7.0 Hz, 1H), 7.66 (dd, J = 8.4 Hz, J = 7.0 Hz, 1H), 7.60 (d, J = 7.7 Hz, 1H), 6.83 (d, J = 7.7 Hz, 1H), 4.76 (s, 2H), 4.66 (s, 2H), 3.34–3.29 (m, 2H), 3.25–3.20 (m, 2H), 2.46 (t, J = 6.6 Hz, 2H), 2.38 (t, J = 6.5 Hz, 2H), 2.23 (s, 6H), 2.21 (s, 6H). ¹³C NMR (150 MHz, DMSO-*d*₆): δ 167.1, 166.4, 150.1, 147.5, 146.9, 136.5, 134.4, 127.3, 125.5, 125.5, 125.3, 123.6, 122.9, 121.9, 97.4, 94.8, 67.8, 57.8, 57.6, 50.5, 44.9, 44.7, 36.7, 36.1. HRMS (ESI) *m/z*: calcd for C₂₆H₃₄N₇O₄⁺ [M+H]⁺: 508.2667; found 508.2664.

2.1.7. General Procedure for the Preparation of Trifluoroacetate Salt of Derivatives 7 Bearing Two Guanidino-Containing Tethers

To a solution of **5** (0.05 mmol) in DMSO (1.5 mL), DIPEA (35 μ L, 0.2 mmol, 4 eq.), followed by 1H-pyrazole-1-carboxamide hydrochloride (22.0 mg, 0.15 mmol, 3 eq.), was added. The reaction mixture was heated for 3 h at 60 °C, cooled to room temperature, diluted with water (2.5 mL), and purified using preparative HPLC, yielding **7**.

Ditrifluoroacetate salt of N-(2-guanidinoethyl)-2-(7-(2-((2-guanidinoethyl)amino)-2-oxoethoxy)-1-oxobenzo[4,5]imidazo[1,2-c]pyrimidin-2(1H)-yl)acetamide **7a**

Starting from **5a**, the title compound was obtained with a yield of 47% as a yellowish amorphous solid. HPLC rt 5.8 min. ¹H NMR (600 MHz, DMSO-*d*₆): δ 9.31 (br s, 1H), 9.25 (br s, 1H), 8.77 (m, 1H), 8.46 (m, 1H), 7.94–7.72 (m, 4H), 7.88 (d, J = 2.4 Hz, 1H), 7.67 (d, J = 8.8 Hz, 1H), 7.61 (d, J = 7.6 Hz, 1H), 7.18 (dd, J = 8.8 Hz, J = 2.4 Hz, 1H), 6.66 (d, J = 7.6 Hz, 1H), 4.64 (s, 2H), 4.58 (s, 2H), 3.33–3.27 (m, 2H), 3.26–3.21 (m, 2H), 3.19–3.13 (m, 4H). ¹³C NMR (150 MHz, DMSO-*d*₆): δ 168.0, 167.0, 157.6, 157.6, 154.1, 148.4, 147.4, 138.7, 137.8, 130.0, 119.1, 114.5, 99.9, 97.1, 67.6, 50.3, 40.3, 40.1, 38.0, 37.4. HRMS (ESI) *m/z*: calcd for C₂₀H₂₈N₁₁O₄⁺ [M+H]⁺: 486.2320; found 486.2319.

Ditrifluoroacetate salt of N-(2-guanidinoethyl)-2-(5-(2-((2-guanidinoethyl)amino)-2-oxoethoxy)-11-oxonaphtho[2',1':4,5]imidazo[1,2-c]pyrimidin-10(11H)-yl)acetamide **7b**

Starting from **5b**, the title compound was obtained with a yield of 50% as a yellowish amorphous solid. HPLC rt 6.5 min. ¹H NMR (600 MHz, DMSO-*d*₆): δ 9.43 (br s, 2H), 8.84 (br s, 1H), 8.58–8.47 (m, 3H), 8.05–7.76 (br s, 4H), 7.88 (s, 1H), 7.75 (dd, J = 8.0 Hz, J = 7.0 Hz, 1H), 7.65 (dd, J = 8.4 Hz, J = 7.0 Hz, 1H), 7.62 (d, J = 7.6 Hz, 1H), 6.82 (d, J = 7.6 Hz, 1H), 4.79 (s, 2H), 4.69 (s, 2H), 3.39–3.36 (m, 2H), 3.28–3.23 (m, 2H), 3.20 (t, J = 5.8 Hz, 2H), 3.19–3.16 (m, 2H). ¹³C NMR (150 MHz, DMSO-*d*₆): δ 167.7, 167.0, 157.7, 150.1, 147.5, 146.9, 136.4, 134.4, 127.3, 125.5, 125.5, 125.4, 123.6, 123.1, 121.9, 97.5, 94.8, 67.7, 50.5, 40.4, 40.1, 38.0, 37.4. HRMS (ESI) *m/z*: calcd for C₂₄H₃₀N₁₁O₄⁺ [M+H]⁺: 536.2477; found 536.2475.

2.1.8. Dihydrochloride Salt of N-(2-Aminoethyl)-2-(5-(2-((2-aminoethyl)amino)-2-oxoethoxy)-11-oxonaphtho[2',1':4,5]imidazo[1,2-c]pyrimidin-10(11H)-yl)acetamide (**5b**·2HCl)

To a suspension of **5b** (90 mg, 0.2 mmol) in CH₃OH (5 mL), 7N aqueous HCl solution (0.2 mL) was added, and the resulting mixture was stirred at room temperature overnight. Then, Et₂O (50 mL) was added dropwise with vigorous stirring, and the formed precipitate was filtered, washed with Et₂O (2 \times 25 mL), and dried in vacuo, yielding **5b**·2HCl as a light beige crystalline solid (94%). M.p. ~165 °C with decomposition. ¹H NMR (600 MHz, D₂O): δ 8.13 (d, J = 8.2 Hz, 1H), 7.96 (d, J = 8.1 Hz, 1H), 7.65 (t, J = 7.4 Hz, 1H), 7.59 (d, J = 7.6 Hz, 1H), 7.58 (t, J = 7.1 Hz, 1H), 7.01 (s, 1H), 6.74 (d, J = 7.6 Hz, 1H), 4.80 (s, 2H, overlaps with DHO), 4.60 (s, 2H), 3.74 (t, J = 6.2 Hz, 2H), 3.70 (t, J = 5.9 Hz, 2H), 3.31 (t, J = 6.2 Hz, 2H), 3.30 (t, J = 5.9 Hz, 2H). ¹³C NMR (150 MHz, D₂O): δ 171.3, 169.3, 150.3, 146.8, 145.8, 138.6, 128.7, 128.0, 126.5, 124.1, 123.2, 122.4, 122.4, 121.1, 96.0, 93.3, 67.0, 51.4, 39.1, 39.0, 37.1, 36.8.

2.2. Cell-Based Assays

2.2.1. Cell Lines

Cell lines MCF7', VA13, A549, and HEK293T were maintained in DMEM/F-12 (Thermo Fisher Scientific, Madison, WI, USA) culture medium containing 10% fetal bovine serum (Thermo Fisher Scientific, Madison, WI, USA), 50 μ g/mL penicillin, and 0.05 mg/mL streptomycin at 37 °C (Thermo Fisher Scientific, Madison, WI, USA) in 5% CO₂. Cells were maintained at 37 °C in a MCO-18AC humidified incubator (Sanyo, Tokyo, Japan) supplied with 5% CO₂. The cell cultures were tested for the absence of mycoplasma and validated by STR.

2.2.2. MTT Assay

The cytotoxicity of the substances was tested using the MTT (3-(4,5-dimethylthiazol-2-yl)2,5-diphenyl tetrazolium bromide) Mosmann assay [23] with some modifications. A

total of 2500 cells per well for the MCF7', HEK293T, and A549 cell lines or 4000 cells per well for the VA13 cell line were plated out in 135 μ L of DMEM-F12 medium (Gibco, USA) in a 96-well plate and incubated in a 5% CO₂ incubator for 20 h without treatment. Then, 15.8 μ L of the corresponding medium-DMSO solutions of the substances being tested was added to the cells in triplicate for each dilution (eight concentrations with three-times dilutions with final concentrations in cells ranging from 0.05 to 100 μ M; the final DMSO concentrations in the medium were 0.5% or less) and incubated for 72 h. Doxorubicin was used as a control substance. Then, the MTT reagent (Paneco LLC, Moscow, Russia) was added to the cells up to the final concentration of 0.5 g/L (10 \times stock solution in PBS was used) and incubated for 1.5 h (MCF7', HEK293T and A549 cells) or 3 h (VA13 cells) at 37 $^{\circ}$ C in the 5% CO₂ incubator. Then, the MTT solution was discarded, and 140 μ L of DMSO (PharmaMed LLC, Moscow, Russia) was added. The plates were agitated on a shaker (120 rpm) to dissolve the formazan. Absorbance was measured using a Victor X5 microplate reader (PerkinElmer, Waltham, MA USA) at a wavelength of 555 nm. The results were used to construct dose–response curves by non-linear regression approximation of the normalized data and to estimate IC_{50Abs} values (IC_{50Abs} is the concentration resulting in two-fold decrease in the number of cells compared to untreated cells) with GraphPad Prism 5 (GraphPad Software Inc., La Jolla, CA, USA).

2.2.3. Apoptosis/Necrosis Assay

A total of 3×10^5 cells per well of the A549 cell line were seeded in 2 mL of DMEM-F12 medium (Gibco, USA) in 6-well plates, and then incubated in the 5% CO₂ incubator for 20 h without treatment. After that, the medium-DMSO solutions of the compounds under test in amounts of 1–33 μ L were added (the DMSO concentrations in the wells were 1.5% or less) and the cells were incubated for 24 h. The cells were collected (a sedimentation procedure was performed at 200–300 g) in 1.5 mL tubes, flushed with PBS, and resuspended in 1X Annexin V binding buffer consisting of 0.01 M HEPES (pH 7.4), 0.14 M NaCl, and 2.5 mM CaCl₂ solution. Then, 5 μ L of Annexin V-FITC (A13201, ThermoFisher, Waltham, MA, USA) was added per 100 μ L of cell solution in a 1 \times binding buffer, and the cells were incubated for 15 min at room temperature. Afterwards, the cells were sedimented, and the solution was replaced with 1X Annexin V binding buffer containing propidium iodide (2.5 μ L of PI (1 mg/mL, ThermoFisher, USA) per 100 μ L of buffer), incubated for 15 min at room temperature. Then, the cells were analyzed with a LongCyte C3090 flow cytometer (Challenbio, Beijing, China) after staining for 2 h.

Caspase 3/7 activation was analyzed with the Muse[®] Caspase-3/7 Kit (Cytex Biosciences, Fremont, CA, USA). The cells were prepared in the same way as in the previous assay, but they were resuspended in 500 μ L of growth medium, followed by staining and analysis of 100 μ L of the suspension in accordance to the manufacturer's protocol.

2.2.4. Cell Cycle Assay

A total of 1×10^5 cells per well of the A549 cell line were seeded in 1 mL of DMEM-F12 medium (Gibco, USA) in a 12-well plate and incubated in the 5% CO₂ incubator for 20 h without treatment. Then, 2 μ L of medium-DMSO solutions of the substances under test (the final DMSO concentrations in the medium were 0.5% or less) was added to the cells and incubated for 24 h. The cells were collected (a sedimentation procedure was performed at 200–300 g) in 1.5 mL tubes, flushed with PBS, and stained with the staining solution (500 μ L, RPMI1640 medium (Gibco, USA), Hoechst-33342 (10 μ g/mL, Invitrogen, Waltham, MA, USA) with TritonX100 (0.1%) and HEPES-KOH (10 mM pH 7.3)) for 15 min at room temperature. The cells were analyzed with a LongCyte C3090 (Challenbio, Beijing, China) or Amnis FlowSight (Luminex, Austin, TX, USA) flow cytometer after staining for 0.5 h.

2.3. Oligonucleotide-Based Assays

2.3.1. FRET-Melting Assay

Oligodeoxyribonucleotides (ODNs) labeled with 6-carboxyfluorescein (FAM) and Black Hole Quencher 1 (BHQ1) at 5'- and 3'-termini, respectively, and unlabeled oligodeoxynucleotide ds26 were purchased from Litekh (Moscow, Russia) (purity > 95%, HPLC). The ODN sequences are presented in Table S1. Solutions of the ODNs (1 μ M) were prepared in 20 mM sodium phosphate buffer, pH 7.4, supplemented with 10 mM KCl (buffer 1), in all cases except VEGF, for which a 5 mM sodium phosphate buffer, pH 7.4, supplemented with 25 mM LiCl (buffer 2) was used. The compounds under test were added to ODN solutions to final concentrations of 1–20 μ M (1:1, 1:2, 1:5, 1:10, or 1:20 ODN:compound ratio). The mixtures were heated to 95 °C for 5 min and then cooled on ice to facilitate the intra-molecular folding of ODN structures. FRET melting curves were obtained using a QuantStudio 5 PCR system (Thermo Fisher Scientific, USA). Changes in fluorescence at 520 nm were recorded every 0.3 °C during stepwise heating of the samples at an average rate of 1.5 °C/min. Melting temperatures were determined from the maxima of first derivatives of the melting curves. For selectivity analysis, labeled G4-forming oligonucleotides were mixed with pre-annealed unlabeled ds26 (G4 and ds26 concentrations: 0.5 μ M and 10 μ M, respectively); then, the compound under test was added to a final concentration of 10 μ M, and the melting experiments were performed as described above.

2.3.2. MST Assay

ODNs labeled with hexachlorofluorescein (HEX) at the 5'-terminus were purchased from Litekh (Russia) (purity > 95%, HPLC). The ODN sequences are presented in Table S2. The pre-annealed 100 nM solution of 5'-HEX-labeled cKit1 ODN in buffer 1, STAT ODN in buffer 1, or VEGF ODN in buffer 2 was mixed 1:1 (*v/v*) with two-fold dilutions of the compound under test in the corresponding buffer supplemented with 5% DMSO and 0.5% Tween 20. The final concentrations of the compounds being tested ranged from 0 to 240 μ M. The mixtures were incubated at room temperature for 10 min prior to measurements. Microscale thermophoresis (MST) curves were recorded using a Monolith NT.115 instrument and standard capillaries (NanoTemper, Germany) at 22 °C in GREEN mode. To calculate K_d values, the dependence of MST data on the concentration of the compound under test was analyzed using MO. Affinity Analysis software (NanoTemper, Germany).

2.4. Dual Luciferase Reporter (DLR) Assay

The HEK293 cells were cultured in a 25-cm² flask until 70–80% confluency was achieved. Once the required density was reached, the cells were transfected with the pC-Kit1 plasmid (Addgene plasmid #118983) using the GenJect-40 reagent (Molox). After transfection for 4 h, the cells were plated into a 96-well plate at a seeding density of 4×10^4 cells/well. Immediately after seeding, various concentrations of **5b** (5, 20, and 50 μ M) were added to the cells. Luciferase activity was measured 24 h after the treatment using the Dual-Glo[®] Luciferase Assay System (Promega, Madison, WI, USA). All assays were performed in triplicate.

2.5. Fluorescent Intercalator Displacement (FID) Assay

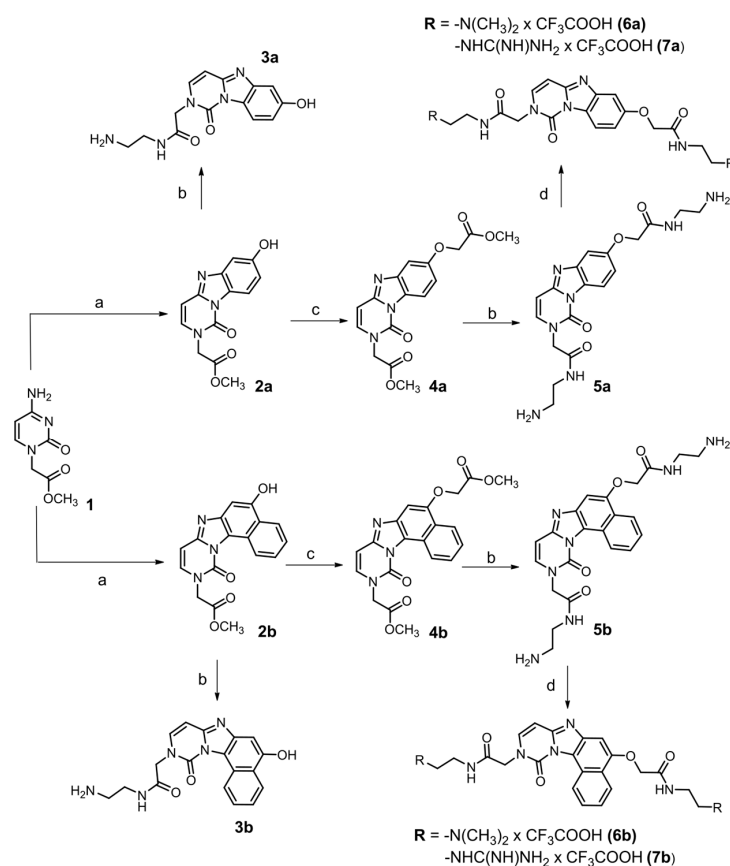
An Ethidium bromide (EtBr) displacement assay was performed in a 40 μ L volume in 384-well black, flat-bottom, polystyrene microtiter plates. Solutions of EtBr in Tris buffer (0.05 M Tris-Cl, pH 7.5, 0.1 M KCl) at a concentration of 6 μ M, 0.016 g/L calf thymus DNA that corresponds to 24 μ M of nucleotide pairs and the compound with final concentrations of 4, 16, 62.5, and 250 μ M dissolved in DMSO (final concentration up to 3%) were prepared. The compound and blank solutions contained the same percentage of DMSO. Once the ethidium bromide solution had been added, the plates were protected from light. The mixtures were

incubated for 15 min, and EtBr fluorescence (545 nm for excitation and 595 nm for emission) was measured using Victor X5 (PerkinElmer).

3. Results and Discussion

3.1. Synthesis of the Compounds

To construct tri- and tetracyclic heteroaromatic systems, we used a reported reaction of 2'-deoxycytidine with 1,4-benzoquinone in sodium acetate buffer (pH 4.5) [19], but started from N1-substituted cytosine **1** (Scheme 1). The treatment of **1** with 1,4-benzoquinone afforded tricyclic derivative **2a**. For the preparation of tetracyclic derivative **2b**, 1,4-naphthoquinone was used with an addition of C₂H₅OH to improve its solubility, and the reaction time was prolonged. Then, **2a–b** were reacted with ethane-1,2-diamine in CH₃OH at 50 °C, affording derivatives **3a–b** with an amino-containing tether. The alkylation of the hydroxyl group in the heteroaromatic moiety of **2a–b** was carried out by the addition of 1,8-diazabicyclo[5.4.0]undec-7-ene (DBU), followed by methyl 2-bromoacetate in CH₂Cl₂, affording intermediates **4a–b**. The subsequent substitution of the methoxy groups in esters **4a–b** with ethane-1,2-diamine in CH₃OH at 50 °C led to ligands **5a–b** bearing two amino-containing tethers. The derivatives **6a–b** were prepared via the reductive methylation of **5a–b** [24]. To convert the amino groups of **5a–b** into the guanidino ones of **7a–b**, a standard guanidinylation agent, 1H-pyrazole-1-carboxamide hydrochloride, was used [25,26].



Scheme 1. Synthesis of benzo- and naphtho-imidazopyrimidinone derivatives. Reagents and conditions: (a) 1,4-benzoquinone, 0.1 M sodium acetate buffer (pH 4.5), 37 °C, 24 h for **2a** (60%) or 1,4-naphthoquinone, 0.1 M sodium acetate buffer (pH 4.5)/C₂H₅OH (2:1, v:v), 50 °C, 7d for **2b** (21%); (b) ethane-1,2-diamine, CH₃OH, 50 °C, 48 h for **3a** (83%), **3b** (80%), **5a** (91%), **5b** (90%); (c) DBU, methyl 2-bromoacetate, CH₂Cl₂, rt, 3h for **4a** (43%) and **4b** (48%); (d) CH₂O, NaCNBH₃, AcOH, MeOH, 0 °C→rt, 2h for **6a** (38%) and **6b** (33%) and 1H-pyrazole-1-carboxamide hydrochloride, DIPEA, DMSO, 60 °C 3h for **7a** (47%) and **7b** (50%).

3.2. Cytotoxicity Assays

The cytotoxicity of benzo- and naphtho-imidazopyrimidinyl derivatives and their intermediates was evaluated via an MTT assay [21], using human breast cancer cell line MCF7' (fast-growth subclone), human lung epithelial carcinoma cell line A549, and non-cancerous lung fibroblast cell line VA13 (Table 1). The cytotoxicity for immortalized human embryonic kidney cell line HEK293T as control non-cancerous fast-growth cells was also studied. Most of the compounds were non- or weakly cytotoxic both for cancerous and control cell lines. The introduction of an additional benzene ring into the heteroaromatic scaffold appears to determine the activity throughout the naphtho series **b**. However, only **5b** with two amino-bearing tethers demonstrated significant cytotoxicity, with the selectivity index (SI) being 3.0 and 17.3 for the VA13/MCF7 and VA13/A549 pairs, respectively (Table 1, Figure 2A). Its congeners carrying dimethylamino and guanidino moieties exhibited weak activity. For some heterocyclic scaffolds, the lower activity of dimethylamino- and guanidino-substituted compounds compared to derivatives with amino groups has been reported [27–29]. Of note, **5b** outperformed commonly used chemotherapy drugs, such as cisplatin, doxorubicin, and 5F-uracil [30,31], in terms of selectivity.

Table 1. Anti-proliferative effects of benzo- and naphtho-imidazopyrimidinone derivatives against HEK293T, MCF7', A549, and VA13 cell lines, and selectivity indexes after 72 h incubation and viability measurement using the Mosmann assay (MTT). VA13 and HEK293T are slow- and fast-growth non-cancerous cell lines, respectively; MCF7' and A549 cell lines are of breast and lung origin, respectively.

Compound	IC ₅₀ abs, μM			SI		
	HEK293T	MCF7'	A549	VA13	VA13/MCF7	VA13/A549
2a	>100	>100	>100	~100	ND	ND
3a	>100	>100	>100	>100	ND	ND
4a	>100	>100	>100	>100	ND	ND
5a	~100	>100	>100	>100	ND	ND
6a	>100	>100	>100	>100	ND	ND
7a	~100	>100	>100	>100	ND	ND
2b	6.1 ± 0.3	30 ± 1	34 ± 2	60 ± 6	2.0	1.7
3b	32 ± 1	95 ± 3	94 ± 5	73 ± 2	0.8	0.8
4b	44 ± 1.9	~100	~100	~100	ND	ND
5b	2.6 ± 0.2	20 ± 2	3.6 ± 0.5	62 ± 5	3.0	17.3
6b	~100	>100	>100	>100	ND	ND
7b	41 ± 4	~100	76 ± 6	~100	ND	ND
Dox	0.02 ± 0.01 ²	0.04 ± 0.02 ²	0.014 ± 0.005 ²	0.11 ± 0.04 ²	3.0	7.9
5F-Uracil	ND	10.0 ± 0.2 ³	4 ± 1 ¹	13.6 ± 0.6 ¹	1.4	3.4
Cisplatin	3.4 ± 1.7 ⁴	5.75 ± 0.02 ⁵	2.69 ± 0.05 ¹	2.04 ± 0.08 ¹	0.4	0.8

ND—not determined^{1–5} Data about cytotoxicity of known drugs were retrieved from¹ [31],² [32],³ [33],⁴ [34], and⁵ [35].

The treatment with **5b** did not cause complete cell death even at high concentrations (Figure 2A), and apoptosis induction is not the main mechanism of action of the compound (Table S3, Figures S1 and S2). We checked if **5b** had cytostatic activity and found that it caused G2 arrest in A549 cells (Table 2, Figure 2B). This effect was significant, though less prominent than after the treatment of cells with the well-established cytostatic drug paclitaxel with G2-arresting activity [36,37].

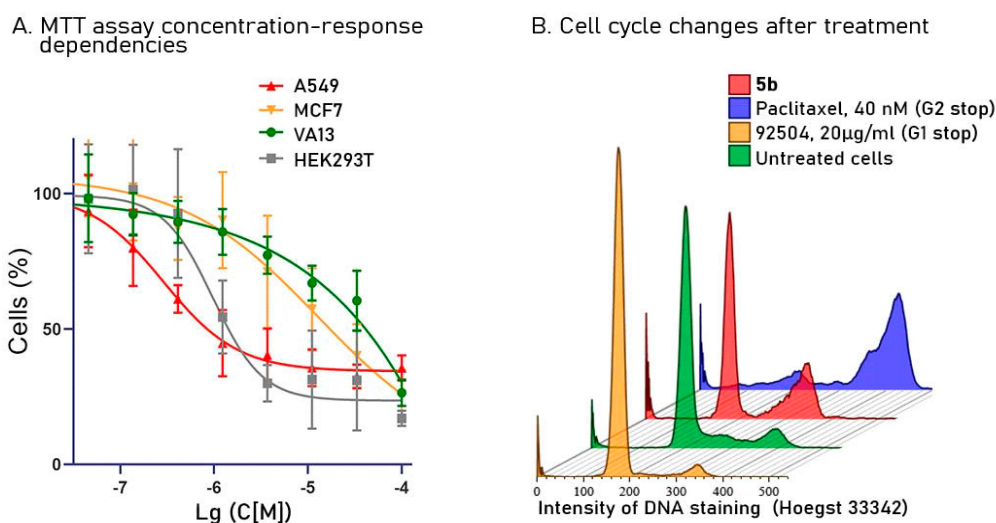


Figure 2. (A) Dose–response dependencies of cytotoxicity for HEK293T, MCF7, A549, and VA13 cell lines after a 72 h treatment with **5b**. (B) Changes in cell cycle distribution of lung cancer cells A549 after a 20 h treatment with **5b**, paclitaxel, and 92504.

Table 2. Cell cycle effects of **5b** and G1 and G2 phase-arresting drugs 92504 and paclitaxel, respectively.

Sample	G1, %	S, %	G2, %
5b	58	6	36
92504 (cause G1-stop)	91	3	6
Paclitaxel (cause G2-stop)	10	8	82
Untreated cells	72	17	11

3.3. Verification of DNA Targets: FRET-Melting and Microscale Thermophoresis (MST) Assays

In an attempt to elucidate the mechanism of action underlying the anti-proliferative properties, we investigated the ability of the most active tetracyclic derivatives to interact with a panel of biologically relevant DNA secondary structures. The non-active tricyclic analogs were used as negative controls. Compound **5b** contains a planar condensed aromatic core and positively charged tethers, allowing for interactions with the DNA duplex leading to DNA damage. In addition, carbazole-based derivatives can stabilize G4s that regulate oncogene transcription and inhibit telomere elongation [38]. Telomeric and c-Myc G4s have previously been reported as the main targets of carbazole-based G4 ligands [3].

Here, we used a FRET-melting assay with FAM/BHQ-labeled ODNs to evaluate the stabilizing effects of the synthesized compounds on the DNA duplex and G4s. The 23-mer hairpin Hair was chosen as a model duplex [39]. In addition to telomeric 22AG [40] and c-Myc [41] G4s, three G4s from the promoters of oncogenes cKit1 [42], STAT [43], and VEGF [44], as well as three imperfect G4s (Ct1, BclI, and 22CTA) [45,46], were also included. To verify a topological preference, if any, the G4 set encompassed various topologies: antiparallel (22CTA and STAT), parallel (cMyc, cKit1, and VEGF), hybrid (22AG) and mixed hybrid/antiparallel (Ct1 and BclI) G4s. Furthermore, three of them, namely, cKit1, STAT, and VEGF, contained long loops that can be involved in the interactions with G4 stabilizers. In order to determine the effective concentration range and roughly evaluate the binding affinity of the compounds to G4 targets, the concentration dependence of the stabilizing effects was analyzed in a series of titration assays (Tables S4 and S5).

The G4/hairpin-stabilizing effects of all compounds are summarized in Figure 3. Both tricyclic and tetracyclic compounds increased the T_m of G4s, but the stabilization of the hairpin was observed only in the naphtho series b. The compounds demonstrated no apparent selectivity for particular types of G4 topologies. The smallest stabilizing effect

was observed for c-Myc G4, which has the highest intrinsic thermal stability (the highest T_m value in the absence of the ligand), in all cases except for the case of 6b. Weak to moderate stabilizing effects were predominantly observed for telomeric (22AG) and imperfect (BclT, 22CTA, and Ct1) G4s, except for the highly efficient stabilizers 5b and 7b. Both tri- and tetracyclic derivatives gave the highest increase in melting temperature for cKit1, STAT, and VEGF G4s. Taking into account that the last three G4s have the longest loops, the efficacy of G4 stabilization could depend on loop–ligand interactions.

Code	T_m °C±1	ΔT_m °C±2 ($T_m^{lig} - T_m^{no\ lig}$)							
		3a	3b	5a	5b	6a	6b	7a	7b
22AG	55	1	6	9	16	6	14	12	23
cMyc	76	1	4	5	12	2	>17	8	16
cKit1	50	3	11	17	24	12	22	19	35
Ct1	39	2	6	10	23	6	17	9	30
BclT	42	0	4	9	18	5	12	10	24
STAT	59	1	10	13	33	13	31	18	23
VEGF	53	1	18	16	31	15	30	21	>43
22CTA	53	1	5	9	18	5	14	12	22
Hair	59	-1	0	3	9	1	8	4	19

Figure 3. Heatmap of the influence of the compounds on the thermal stability of DNA targets. The concentrations of the compounds and the targets were 1 and 20 μ M, respectively. For all targets except VEGF, buffer 1 (20 mM sodium phosphate, pH 7.4, 10 mM KCl) was used. For VEGF, buffer 2 (5 mM sodium phosphate, pH 7.4, 25 mM LiCl) was used.

Tricyclic derivative 3a with a positively charged amino-containing tether demonstrated no stabilizing effect. Among the di-substituted tricyclic derivatives, guanidylated 7a exhibited the highest stabilizing effect, while 6a with dimethylamino-bearing arms showed the lowest one. A similar dependence of the effect on the type and number of tethered groups ($3b < 5b < 6b < 7b$ in most cases) was observed among the tetracyclic compounds.

The introduction of an additional benzene ring into the benzoimidazopyrimidinone scaffold had a positive impact on the stabilization of the G4s and the hairpin, presumably due to additional stacking contacts with outer G tetrads or canonical Watson–Crick base pairs. Mono-substituted compounds were the weakest stabilizers in both series, suggesting that the number of positively charged terminal groups influences stabilization efficacy, presumably due to electrostatic interactions with the sugar-phosphate backbone. The superiority of the guanidylated derivatives can be explained by the high pK_a value of the guanidino group [47]. The lower efficacy of N-dimethylated derivatives can result from charge shielding and steric hindrance [27].

In summary, the tetracyclic molecules exhibited a more pronounced stabilization of both G4s and duplex DNA, that is mostly consistent with their anti-proliferative activity. In contrast, the tricyclic derivatives that were inactive in MTT assays demonstrated lower G4-stabilizing effects and no impact on duplex thermal stability.

To assess G4 vs. duplex selectivity, we chose five G4 targets that were stabilized most effectively in the previous assay, and performed FRET melting in the presence of derivatives and a competitor—unlabeled hairpin ds26 at a 20-fold excess relative to G4 (Figure 4). The mono-substituted derivative 3a was excluded due to the lack of effect. For all investigated compounds, except for the mono-substituted tetracyclic compound 3b, the melting point of VEGF decreased significantly in the presence of ds26. Regarding tricyclic molecules, the stabilizing effect on 22AG, 22CTA, STAT, and cKit1 G4s remained almost unchanged, with the derivatives demonstrating a preference for these G4 targets over duplex DNA. The stabilizing effects of di-substituted tetracyclic compounds mainly decreased in the presence of the competitor. Surprisingly, a high stabilizing effect was

observed for STAT in the presence of ds26, which might be explained by the formation of a triple G4/ds26/derivative complex. cKit1 G4 can be highlighted as a preferred target for tetracyclic derivatives, but, upon entering the cells, they can target both telomeric G4 and duplex DNA due to their high abundance.

Code	$\Delta T_m^{\circ C \pm 2} (T_m^{G4} - T_m^{G4+ds26})$						
	3b	5a	5b	6a	6b	7a	7b
22AG	2	2	5	0	4	1	8
cKit1	3	0	-1	0	-2	1	-6
STAT	3	0	-24	1	-10	1	ND
VEGF	2	9	25	8	9	11	52
22CTA	3	0	7	-1	6	1	14

Figure 4. Heatmap of changes in the G4-stabilizing effects of the compounds in the presence of duplex DNA. ND—not determined. The concentrations of the compounds, ds26, and the targets were 10 μ M, 10 μ M, and 0.5 μ M, respectively. Buffer 1 (20 mM sodium phosphate, pH 7.4, 10 mM KCl) was used for all targets, and buffer 2 (5 mM sodium phosphate, pH 7.4, 25 mM LiCl) was used for VEGF.

For the most promising compounds, the dissociation constants (K_d) of their complexes with proto-oncogenic G4s STAT, VEGF, and cKit1 were determined using microscale thermophoresis (MST) assays with 5'-HEX-labeled G4 ODNs. The results are presented in Figure 5. The K_d values of 3b/cKit, 5b/cKit, 3b/STAT, and 6a/STAT were in the submicromolar range, and the rest of the complexes tested showed micromolar K_d . Despite causing only a moderate increase in G4 T_m , 3b turned out to be the most efficient G4 binder.

Code	K_d, μ M						
	3b	5a	5b	6a	6b	7a	7b
STAT	0.5	5.1		0.4			
cKit1	0.6	5.6	0.5	1.9	2.6		3.1
VEGF					1.3	4.6	

Figure 5. Heatmap of the dissociation constants K_d of G4:derivative complexes according to MST. ND—not determined.

In order to assess the impact of 5b on cKit expression, a DLR assay with the pC-Kit1 plasmid (Addgene plasmid #118983) that contains two luciferase genes (Renilla/Firefly) was performed. The expression of Renilla is controlled by the c-Kit promoter containing the cKit1 G4-forming sequence, while the expression of Firefly is under control by a non-G4-forming promoter sequence (the HSV TK promoter). After transfection of the plasmid into HEK293T cells for 4 h, followed by a 24 h treatment with 5b, no significant changes in Renilla/Firefly expression ratio compared with the control were observed (Figure S3), suggesting that G4 in the cKit promoter region is not the main target of 5b.

According to the FRET-melting assay, there is evidence for interactions of 5b with DNA structures. The FID assay demonstrated that 5b is a DNA intercalator, though an order of magnitude weaker one than EtBr (Figure S4).

The problem with DNA-targeting compounds is adverse effects and common toxicity in combination with a low selectivity of action. The aims of this study were to evaluate the prospects for further study of this class of derivatives; and to determine whether it is necessary to synthesize additional compounds of this class, study their detailed molecular mechanism, and conduct comprehensive studies in animal models. To evaluate the

prospects of 5b for further application *in vivo*, we prepared its water-soluble dihydrochloride salt 5b·2HCl (see Section 2.1. Chemical synthesis) and performed tolerance tests on mice. Compound 5b·2HCl up to 20 mg/kg did not demonstrate acute toxic effects and caused no changes in mice behavior or decrease in body weight after a 72 h treatment. The results support the prospects of further search for the cellular targets and evaluation *in vivo*. Hopefully, the unraveling of the molecular target of 5b will be accomplished in the future.

4. Conclusions

Novel derivatives of benzo[4,5]- and naphtho[2',1':4,5]imidazo[1,2-c]pyrimidinones were synthesized and evaluated as anti-proliferative agents. Tetracyclic compound 5b with two amino-containing tethers inhibited metabolic activity in the low-micromolar range, with notable selectivity for cancerous and fast-growing cells; however, it did not cause complete cell death. In attempt to explore its mechanism of action, the biological properties of 5b were further studied. A cell cycle assay demonstrated that 5b causes G2 arrest without inducing apoptosis. The interaction of the compounds with DNA targets was of particular interest, and FRET-melting and MST experiments revealed that both benzo[4,5]- and naphtho[2',1':4,5]imidazo[1,2-c]pyrimidinones can bind and stabilize G4s, but only the latter can interact with the DNA duplex. A dual luciferase reporter assay showed that 5b does not regulate gene expression under control by the promoter harboring the cKit1 G4-forming sequence. In contrast, an FID assay revealed the intercalating properties of 5b that could be partly responsible for its anti-proliferative activity. Finally, a water-soluble dihydrochloride salt of 5b up to 20 mg/kg was shown not to be toxic for mice after a 72 h treatment. Here, we have demonstrated the first evidence that naphtho[2',1':4,5]imidazo[1,2-c]pyrimidinone derivative is a DNA-targeting agent that causes cell cycle halting and possesses selectivity for cancer cell lines. Thus, the lead compound looks promising for further investigation; however, the discovery of its molecular targets is necessary.

Supplementary Materials: The following supporting information can be downloaded at: <https://www.mdpi.com/article/10.3390/biom13111669/s1>, Figure S1: Determination of the mode of cell death using Annexin-V and PI staining and flow cytometric analysis; Figure S2: Determination of the mode of cell death using caspase 3/7 staining and flow cytometric analysis; Figure S3: The dual luciferase reporter assay using the pC-Kit1 plasmid; Figure S4: The EtBr displacement assay data for 5b (4, 16, 62.5, 250 μ M) demonstrates intercalation into DNA helix, Acridin-9-amine was used as a control sample; Table S1: Sequences of the ODNs used in FRET-melting assays; Table S2: Sequences of the ODNs used in the MST study; Table S3: Determination of the mode of cell death by 5b using Annexin-V and PI staining and flow cytometric analysis; Table S4: Titration of DNA-targets with the benzo-imidazopyrimidinone derivatives; Table S5: Titration of DNA-targets with the naphtho-imidazopyrimidinone derivatives.

Author Contributions: Conceptualization, A.A.; methodology, V.P., D.S., A.V. and A.A.; investigation, P.K., N.D., S.L., Y.K., V.A., A.S., A.K., A.C., V.P., E.E.-S., A.E.-S. and E.B.; writing—original draft preparation, P.K., D.S., A.V., N.D. and A.A.; writing—review and editing, P.K., D.S., A.V. and A.A.; visualization, P.K., D.S., and A.A.; funding acquisition, D.S. and V.P. All authors have read and agreed to the published version of the manuscript.

Funding: The work was supported by the Russian Science Foundation (RSF grant 22-14-00099). The animal experiments were supported by the State Program of the Ministry of Science and Higher Education of the Russian Federation (no. 075-01551-23-00; FSSF-2023-0006).

Institutional Review Board Statement: Not applicable.

Informed Consent Statement: Not applicable.

Data Availability Statement: Data are contained within the article and supplementary materials.

Acknowledgments: The authors are grateful to K. Lyamzaev and A. Ferberg for assistance with flow cytometry facilities provided by the Moscow State University Development Program PNR5 and Helicon Company. The authors are also grateful to A. Korshun for a fruitful discussion of the manuscript.

Conflicts of Interest: The authors declare no conflict of interest.

References

1. Mattiuzzi, C.; Lippi, G. Current Cancer Epidemiology. *J. Epidemiol. Glob. Health* **2019**, *9*, 217. [[CrossRef](#)] [[PubMed](#)]
2. Anand, U.; Dey, A.; Chandel, A.K.S.; Sanyal, R.; Mishra, A.; Pandey, D.K.; De Falco, V.; Upadhyay, A.; Kandimalla, R.; Chaudhary, A.; et al. Cancer Chemotherapy and beyond: Current Status, Drug Candidates, Associated Risks and Progress in Targeted Therapeutics. *Genes Dis.* **2023**, *10*, 1367–1401. [[CrossRef](#)] [[PubMed](#)]
3. Gluszyńska, A. Biological Potential of Carbazole Derivatives. *Eur. J. Med. Chem.* **2015**, *94*, 405–426. [[CrossRef](#)] [[PubMed](#)]
4. Li, D.; Yang, R.; Wu, J.; Zhong, B.; Li, Y. Comprehensive Review of α -Carboline Alkaloids: Natural Products, Updated Synthesis, and Biological Activities. *Front. Chem.* **2022**, *10*, 988327. [[CrossRef](#)]
5. Sha, F.; Tao, Y.; Tang, C.-Y.; Zhang, F.; Wu, X.-Y. Construction of Benzo[*c*]Carbazoles and Their Antitumor Derivatives through the Diels–Alder Reaction of 2-Alkenylindoles and Arynes. *J. Org. Chem.* **2015**, *80*, 8122–8133. [[CrossRef](#)]
6. Dai, J.; Dan, W.; Zhang, Y.; Wang, J. Recent Developments on Synthesis and Biological Activities of γ -Carboline. *Eur. J. Med. Chem.* **2018**, *157*, 447–461. [[CrossRef](#)]
7. Abinaya, R.; Srinath, S.; Soundarya, S.; Sridhar, R.; Balasubramanian, K.K.; Baskar, B. Recent Developments on Synthesis Strategies, SAR Studies and Biological Activities of β -Carboline Derivatives—An Update. *J. Mol. Struct.* **2022**, *1261*, 132750. [[CrossRef](#)]
8. Alekseyev, R.S.; Kurkin, A.V.; Yurovskaya, M.A. γ -Carbolines and Their Hydrogenated Derivatives. 1. Aromatic γ -Carbolines: Methods of Synthesis, Chemical and Biological Properties (Review). *Chem. Heterocycl. Compd.* **2009**, *45*, 889–925. [[CrossRef](#)]
9. Chen, J.; Dong, X.; Liu, T.; Lou, J.; Jiang, C.; Huang, W.; He, Q.; Yang, B.; Hu, Y. Design, Synthesis, and Quantitative Structure–Activity Relationship of Cytotoxic γ -Carboline Derivatives. *Bioorg. Med. Chem.* **2009**, *17*, 3324–3331. [[CrossRef](#)]
10. Chen, J.; Liu, T.; Wu, R.; Lou, J.; Cao, J.; Dong, X.; Yang, B.; He, Q.; Hu, Y. Design, Synthesis, and Biological Evaluation of Novel N- γ -Carboline Arylsulfonamides as Anticancer Agents. *Bioorg. Med. Chem.* **2010**, *18*, 8478–8484. [[CrossRef](#)]
11. Huang, F.-C.; Chang, C.-C.; Lou, P.-J.; Kuo, I.-C.; Chien, C.-W.; Chen, C.-T.; Shieh, F.-Y.; Chang, T.-C.; Lin, J.-J. G-Quadruplex Stabilizer 3,6-Bis(1-Methyl-4-Vinylpyridinium)Carbazole Diodide Induces Accelerated Senescence and Inhibits Tumorigenic Properties in Cancer Cells. *Mol. Cancer Res.* **2008**, *6*, 955–964. [[CrossRef](#)] [[PubMed](#)]
12. Fossé, P.; René, B.; Saucier, J.-M.; Chi Hung, N.; Bisagni, E.; Paoletti, C. Stimulation by γ -Carboline Derivatives (Simplified Analogues of Antitumor Ellipticines) of Site Specific DNA Cleavage by Calf DNA Topoisomerase II. *Biochem. Pharmacol.* **1990**, *39*, 669–676. [[CrossRef](#)] [[PubMed](#)]
13. Li, P.-H.; Jiang, H.; Zhang, W.-J.; Li, Y.-L.; Zhao, M.-C.; Zhou, W.; Zhang, L.-Y.; Tang, Y.-D.; Dong, C.-Z.; Huang, Z.-S.; et al. Synthesis of Carbazole Derivatives Containing Chalcone Analogs as Non-Intercalative Topoisomerase II Catalytic Inhibitors and Apoptosis Inducers. *Eur. J. Med. Chem.* **2018**, *145*, 498–510. [[CrossRef](#)] [[PubMed](#)]
14. Huang, F.-C.; Chang, C.-C.; Wang, J.-M.; Chang, T.-C.; Lin, J.-J. Induction of Senescence in Cancer Cells by the G-Quadruplex Stabilizer, BMVC4, Is Independent of Its Telomerase Inhibitory Activity: Telomerase-Independent Senescence Induced by BMVC4. *Br. J. Pharmacol.* **2012**, *167*, 393–406. [[CrossRef](#)]
15. Panda, D.; Debnath, M.; Mandal, S.; Bessi, I.; Schwalbe, H.; Dash, J. A Nucleus-Imaging Probe That Selectively Stabilizes a Minor Conformation of c-MYC G-Quadruplex and Down-Regulates c-MYC Transcription in Human Cancer Cells. *Sci. Rep.* **2015**, *5*, 13183. [[CrossRef](#)]
16. Bisagni, E.; Nguyen Chi, H.; Pierre, A.; Pepin, O.; De Cointet, P.; Gros, P. 1-Amino-Substituted 4-Methyl-5H-Pyrido[4,3-*b*]Indoles (Gamma-Carbolines) as Tricyclic Analogues of Ellipticines: A New Class of Antineoplastic Agents. *J. Med. Chem.* **1988**, *31*, 398–405. [[CrossRef](#)]
17. Janin, Y.L.; Carrez, D.; Riou, J.-F.; Bisagni, E. Synthesis and Biological Properties of New Benz(h)Isoquinoline Derivatives. *Chem. Pharm. Bull.* **1994**, *42*, 892–895. [[CrossRef](#)]
18. Hu, L.; Li, Z.; Li, Y.; Qu, J.; Ling, Y.-H.; Jiang, J.; Boykin, D.W. Synthesis and Structure–Activity Relationships of Carbazole Sulfonamides as a Novel Class of Antimitotic Agents Against Solid Tumors. *J. Med. Chem.* **2006**, *49*, 6273–6282. [[CrossRef](#)]
19. Chenna, A.; Singer, B. Large Scale Synthesis of P-Benzoquinone-2'-Deoxycytidine and p-Benzoquinone-2'-Deoxyadenosine Adducts and Their Site-Specific Incorporation into DNA Oligodeoxyribonucleotides. *Chem. Res. Toxicol.* **1995**, *8*, 865–874. [[CrossRef](#)]
20. Sharma, V.; Gupta, M.; Kumar, P.; Sharma, A. A Comprehensive Review on Fused Heterocyclic as DNA Intercalators: Promising Anticancer Agents. *Curr. Pharm. Des.* **2021**, *27*, 15–42. [[CrossRef](#)]
21. Duarte, A.R.; Cadoni, E.; Ressurreição, A.S.; Moreira, R.; Paulo, A. Design of Modular G-quadruplex Ligands. *ChemMedChem* **2018**, *13*, 869–893. [[CrossRef](#)] [[PubMed](#)]

22. Schwergold, C.; Depecker, G.; Giorgio, C.D.; Patino, N.; Jossinet, F.; Ehresmann, B.; Terreux, R.; Cabrol-Bass, D.; Condom, R. Cyclic PNA Hexamer-Based Compound: Modelling, Synthesis and Inhibition of the HIV-1 RNA Dimerization Process. *Tetrahedron* **2002**, *58*, 5675–5687. [[CrossRef](#)]
23. Mosmann, T. Rapid Colorimetric Assay for Cellular Growth and Survival: Application to Proliferation and Cytotoxicity Assays. *J. Immunol. Methods* **1983**, *65*, 55–63. [[CrossRef](#)] [[PubMed](#)]
24. Paquette, L.A.; Mitzel, T.M.; Isaac, M.B.; Crasto, C.F.; Schomer, W.W. Diastereoselection during 1,2-Addition of the Allylindium Reagent to α -Thia and α -Amino Aldehydes in Aqueous and Organic Solvents. *J. Org. Chem.* **1997**, *62*, 4293–4301. [[CrossRef](#)]
25. Bernatowicz, M.S.; Wu, Y.; Matsueda, G.R. 1H-Pyrazole-1-Carboxamide Hydrochloride an Attractive Reagent for Guanylation of Amines and Its Application to Peptide Synthesis. *J. Org. Chem.* **1992**, *57*, 2497–2502. [[CrossRef](#)]
26. Maier, M.A.; Barber-Peoc'h, I.; Manoharan, M. Postsynthetic Guanidinylation of Primary Amino Groups in the Minor and Major Grooves of Oligonucleotides. *Tetrahedron Lett.* **2002**, *43*, 7613–7616. [[CrossRef](#)]
27. Lizunova, S.A.; Tsvetkov, V.B.; Skvortsov, D.A.; Kamzeeva, P.N.; Ivanova, O.M.; Vasilyeva, L.A.; Chistov, A.A.; Belyaev, E.S.; Khrulev, A.A.; Vedekhina, T.S.; et al. Anticancer Activity of G4-Targeting Phenoxazine Derivatives in Vitro. *Biochimie* **2022**, *201*, 43–54. [[CrossRef](#)]
28. Müller, S.; Sanders, D.A.; Di Antonio, M.; Matsis, S.; Riou, J.-F.; Rodriguez, R.; Balasubramanian, S. Pyridostatin Analogues Promote Telomere Dysfunction and Long-Term Growth Inhibition in Human Cancer Cells. *Org. Biomol. Chem.* **2012**, *10*, 6537. [[CrossRef](#)]
29. Shchekotikhin, A.E.; Glazunova, V.A.; Dezhenkova, L.G.; Luzikov, Y.N.; Sinkevich, Y.B.; Kovalenko, L.V.; Buyanov, V.N.; Balzarini, J.; Huang, F.-C.; Lin, J.-J.; et al. Synthesis and Cytotoxic Properties of 4,11-Bis[(Aminoethyl)Amino]Anthra[2,3-b]Thiophene-5,10-Diones, Novel Analogues of Antitumor Anthracene-9,10-Diones. *Bioorg. Med. Chem.* **2009**, *17*, 1861–1869. [[CrossRef](#)]
30. Krasnovskaya, O.O.; Akasov, R.A.; Spector, D.V.; Pavlov, K.G.; Bublely, A.A.; Kuzmin, V.A.; Kostyukov, A.A.; Khaydukov, E.V.; Lopatukhina, E.V.; Semkina, A.S.; et al. Photoinduced Reduction of Novel Dual-Action Riboplatin Pt(IV) Prodrug. *ACS Appl. Mater. Interfaces* **2023**, *15*, 12882–12894. [[CrossRef](#)]
31. Skvortsov, D.A.; Kalinina, M.A.; Zhirkina, I.V.; Vasilyeva, L.A.; Ivanenkov, Y.A.; Sergiev, P.V.; Dontsova, O.A. From Toxicity to Selectivity: Coculture of the Fluorescent Tumor and Non-Tumor Lung Cells and High-Throughput Screening of Anticancer Compounds. *Front. Pharmacol.* **2021**, *12*, 713103. [[CrossRef](#)] [[PubMed](#)]
32. Novotortsev, V.K.; Kukushkin, M.E.; Tafeenko, V.A.; Skvortsov, D.A.; Kalinina, M.A.; Timoshenko, R.V.; Chmelyuk, N.S.; Vasilyeva, L.A.; Tarasevich, B.N.; Gorelkin, P.V.; et al. Dispirooxindoles Based on 2-Selenoxo-Imidazolidin-4-Ones: Synthesis, Cytotoxicity and ROS Generation Ability. *Int. J. Mol. Sci.* **2021**, *22*, 2613. [[CrossRef](#)] [[PubMed](#)]
33. Loo, W.T.Y.; Sasano, H.; Chow, L.W.C. Evaluation of Therapeutic Efficacy of Capecitabine on Human Breast Carcinoma Tissues and Cell Lines in Vitro. *Biomed. Pharmacother.* **2007**, *61*, 553–557. [[CrossRef](#)]
34. Pagliaricci, N.; Pettinari, R.; Marchetti, F.; Pettinari, C.; Cappellacci, L.; Tombesi, A.; Cuccioloni, M.; Hadiji, M.; Dyson, P.J. Potent and Selective Anticancer Activity of Half-Sandwich Ruthenium and Osmium Complexes with Modified Curcuminoid Ligands. *Dalton Trans.* **2022**, *51*, 13311–13321. [[CrossRef](#)] [[PubMed](#)]
35. Suberu, J.O.; Romero-Canelón, I.; Sullivan, N.; Lapkin, A.A.; Barker, G.C. Comparative Cytotoxicity of Artemisinin and Cisplatin and Their Interactions with Chlorogenic Acids in MCF7 Breast Cancer Cells. *ChemMedChem* **2014**, *9*, 2791–2797. [[CrossRef](#)]
36. Zhu, Z.; Chen, D.; Zhang, W.; Zhao, J.; Zhi, L.; Huang, F.; Ji, H.; Zhang, J.; Liu, H.; Zou, L.; et al. Modulation of Alternative Splicing Induced by Paclitaxel in Human Lung Cancer. *Cell Death Dis.* **2018**, *9*, 491. [[CrossRef](#)]
37. Shu, C.-H.; Yang, W.K.; Shih, Y.-L.; Kuo, M.-L.; Huang, T.-S. Cell Cycle G2/M Arrest and Activation of Cyclin-Dependent Kinases Associated with Low-Dose Paclitaxel-Induced Sub-G1 Apoptosis. *Apoptosis* **1997**, *2*, 463–470. [[CrossRef](#)]
38. Cimino-Reale, G.; Zaffaroni, N.; Folini, M. Emerging Role of G-Quadruplex DNA as Target in Anticancer Therapy. *Curr. Pharm. Des.* **2017**, *22*, 6612–6624. [[CrossRef](#)]
39. Tsvetkov, V.B.; Varizhuk, A.M.; Lizunova, S.A.; Nikolenko, T.A.; Ivanov, I.A.; Severov, V.V.; Belyaev, E.S.; Shitikov, E.A.; Pozmogova, G.E.; Aralov, A.V. Phenoxazine-Based Scaffold for Designing G4-Interacting Agents. *Org. Biomol. Chem.* **2020**, *18*, 6147–6154. [[CrossRef](#)]
40. Dai, J.; Carver, M.; Punchihewa, C.; Jones, R.A.; Yang, D. Structure of the Hybrid-2 Type Intramolecular Human Telomeric G-Quadruplex in K⁺ Solution: Insights into Structure Polymorphism of the Human Telomeric Sequence. *Nucleic Acids Res.* **2007**, *35*, 4927–4940. [[CrossRef](#)]
41. Phan, A.T.; Modi, Y.S.; Patel, D.J. Propeller-Type Parallel-Stranded G-Quadruplexes in the Human *c-Myc* Promoter. *J. Am. Chem. Soc.* **2004**, *126*, 8710–8716. [[CrossRef](#)] [[PubMed](#)]
42. Phan, A.T.; Kuryavyi, V.; Burge, S.; Neidle, S.; Patel, D.J. Structure of an Unprecedented G-Quadruplex Scaffold in the Human *c-Kit* Promoter. *J. Am. Chem. Soc.* **2007**, *129*, 4386–4392. [[CrossRef](#)] [[PubMed](#)]
43. Lin, S.; Xu, M.; Yuan, G. Study of STAT3 G-Quadruplex Folding Patterns by CD Spectroscopy and Molecular Modeling. *Chin. Chem. Lett.* **2012**, *23*, 329–331. [[CrossRef](#)]
44. Turaev, A.V.; Tsvetkov, V.B.; Tankevich, M.V.; Smirnov, I.P.; Aralov, A.V.; Pozmogova, G.E.; Varizhuk, A.M. Benzothiazole-Based Cyanines as Fluorescent “Light-up” Probes for Duplex and Quadruplex DNA. *Biochimie* **2019**, *162*, 216–228. [[CrossRef](#)]
45. Varizhuk, A.; Ischenko, D.; Tsvetkov, V.; Novikov, R.; Kulemin, N.; Kaluzhny, D.; Vlasenok, M.; Naumov, V.; Smirnov, I.; Pozmogova, G. The Expanding Repertoire of G4 DNA Structures. *Biochimie* **2017**, *135*, 54–62. [[CrossRef](#)]

46. Lim, K.W.; Alberti, P.; Guédin, A.; Lacroix, L.; Riou, J.-F.; Royle, N.J.; Mergny, J.-L.; Phan, A.T. Sequence Variant (CTAGGG)_n in the Human Telomere Favors a G-Quadruplex Structure Containing a G·C·G·C Tetrad. *Nucleic Acids Res.* **2009**, *37*, 6239–6248. [[CrossRef](#)]
47. Xu, B.; Jacobs, M.I.; Kostko, O.; Ahmed, M. Guanidinium Group Remains Protonated in a Strongly Basic Arginine Solution. *ChemPhysChem* **2017**, *18*, 1503–1506. [[CrossRef](#)]

Disclaimer/Publisher's Note: The statements, opinions and data contained in all publications are solely those of the individual author(s) and contributor(s) and not of MDPI and/or the editor(s). MDPI and/or the editor(s) disclaim responsibility for any injury to people or property resulting from any ideas, methods, instructions or products referred to in the content.